

## Impact of perturbations to nitrogen oxide emissions from global aviation

Marcus O. Köhler,<sup>1,3</sup> Gaby Rädcl,<sup>2</sup> Olivier Dessens,<sup>1,3</sup> Keith P. Shine,<sup>2</sup> Helen L. Rogers,<sup>1,3</sup> Oliver Wild,<sup>1,4</sup> and John A. Pyle<sup>1,3,5</sup>

Received 9 July 2007; revised 22 November 2007; accepted 1 February 2008; published 10 June 2008.

[1] The atmospheric response to perturbations in  $\text{NO}_x$  emissions from global air traffic is investigated by performing a coherent set of sensitivity experiments. The importance of cruise altitude, size of the emission perturbation and geographical distribution of emissions is systematically analyzed using two global chemistry transport models and an off-line radiative transfer model.  $\text{NO}_x$  emissions from a contemporary aircraft inventory have been used to assess the impact of global air traffic on ozone and methane. In further experiments the  $\text{NO}_x$  emissions are perturbed, in turn, in 16 cruise altitude bands between 5 and 15 km altitude. In the p-TOMCAT model we diagnose an annual mean ozone increase of up to 6 ppbv and a decrease in the methane lifetime of 3% due to global air traffic in 2002. Associated radiative forcings of  $30 \text{ mWm}^{-2}$  for ozone and  $-19 \text{ mWm}^{-2}$  for methane are diagnosed; a simple method is used to estimate the forcing due to the methane-induced ozone change and this yields an additional  $-11 \text{ mWm}^{-2}$ . Results show that up to the tropopause, ozone production efficiency and resulting impacts increase per emitted mass of  $\text{NO}_x$  with the altitude of the perturbation. Between 11 and 15 km we find that the geographical location of the  $\text{NO}_x$  emissions plays a crucial role in the potential  $\text{O}_3$  impact and lifetime change of  $\text{CH}_4$ . We show that changes in flight routing in this altitude range can have significant consequences for  $\text{O}_3$  and  $\text{CH}_4$  concentrations. Overall, we demonstrate a linear relationship in the atmospheric response to small emission changes which can be used to predict the importance of perturbations about the reference aircraft emissions profile, provided the geographical distribution of the emissions is not altered significantly.

**Citation:** Köhler, M. O., G. Rädcl, O. Dessens, K. P. Shine, H. L. Rogers, O. Wild, and J. A. Pyle (2008), Impact of perturbations to nitrogen oxide emissions from global aviation, *J. Geophys. Res.*, 113, D11305, doi:10.1029/2007JD009140.

### 1. Introduction

[2] Nitrogen oxides ( $\text{NO}_x = \text{NO} + \text{NO}_2$ ) play an important role in the chemical formation of ozone ( $\text{O}_3$ ) in the troposphere and lower stratosphere [Crutzen, 1973; Liu *et al.*, 1987]. Enhanced  $\text{NO}_x$  can increase  $\text{O}_3$  concentrations resulting in a positive radiative forcing. The resulting enhancement of the oxidizing capacity of the troposphere reduces the lifetime of methane ( $\text{CH}_4$ ) which leads to a negative forcing [Fuglestedt *et al.*, 1999; Wild *et al.*, 2001; Stevenson *et al.*, 2004] and the reduced methane itself also leads to a reduction in ozone. Therefore emissions of nitrogen oxides act as an indirect forcing agent by altering the abundance of chemically active greenhouse gases.

Global air traffic represents a major source of  $\text{NO}_x$  throughout the free troposphere [e.g., Brasseur *et al.*, 1998; IPCC, 1999; Sausen *et al.*, 2005], together with other sources from lightning [e.g., Chameides *et al.*, 1977], downward transport from the stratosphere [e.g., Lamarque *et al.*, 1996] and convective uplift from polluted regions close to the surface [e.g., Brunner *et al.*, 1998]. Quantification of the impact of aircraft  $\text{NO}_x$  however remains difficult as the chemical formation of ozone is strongly dependent on the ambient background concentrations of the oxides of both hydrogen and nitrogen and of volatile organic compounds [Jaeglé *et al.*, 1998a; IPCC, 1999].

[3] Several recent studies have investigated the possibility of minimizing the impact of aircraft  $\text{NO}_x$  emissions on ozone and methane through changes in routing or cruise altitude [Grewe *et al.*, 2002a; Isaksen, 2003]. Their findings have shown that such operational changes have an impact both on atmospheric composition and related radiative forcings [Grewe *et al.*, 2002a; Gauss *et al.*, 2006a; Stordal *et al.*, 2006]. These studies investigated the sensitivity of the atmospheric impact to a shift in the flight altitude of the global aircraft fleet. Although it is possible to determine the net impacts the identification and quantification of individual processes remains difficult.

<sup>1</sup>Centre for Atmospheric Science, Department of Chemistry, University of Cambridge, Cambridge, UK.

<sup>2</sup>Department of Meteorology, University of Reading, Reading, UK.

<sup>3</sup>Institute for Aviation and the Environment, University of Cambridge, Cambridge, UK.

<sup>4</sup>Now at the Department of Environmental Science, Lancaster University, Lancaster, UK.

<sup>5</sup>NCAS-Climate, University of Cambridge, Cambridge, UK.

[4] In this study we have adopted a more systematic approach by investigating the atmosphere's sensitivity to perturbations of a range of key emission parameters. The change in global greenhouse gas concentrations and the associated radiative impacts following the  $\text{NO}_x$  emission perturbations have been considered using two 3-dimensional global chemistry transport models and an off-line radiation code. This study also includes an explicit calculation of the longer term impact of  $\text{NO}_x$  emission perturbations on methane. Aircraft  $\text{NO}_x$  emissions are increased by 5%, 10% and 20% within a selection of designated cruise altitude bands. Such small increases in emissions could represent the introduction of a new aircraft to the existing commercial fleet or changes in air traffic demand. Above 11 km altitude, where the geographical coverage of emissions changes rapidly with altitude, we also investigate the impact of a varying geographical distribution of the emissions by perturbing the geographical coverage at a given cruise altitude band while maintaining the total emitted amount. A more quantitative account of the methodology used is described in section 3. This methodology allows us to investigate the atmospheric sensitivity to aircraft  $\text{NO}_x$  as a function of location, altitude, and magnitude of the emission perturbation. These emission perturbations form a coherent set of sensitivity experiments from which we aim to establish a relationship between the change in the emission parameter and the response of the atmosphere. A related study [Rädel and Shine, 2008] investigates, in a similar manner, the impact of changes in flight altitude on contrail radiative forcing.

[5] The following section describes the chemistry transport models used and the methodology adopted to calculate the indirect  $\text{NO}_x$  effects on methane. Section 3 outlines the experiments. The effects of aircraft emissions on ozone and methane and the sensitivity to cruise altitude are discussed in sections 4 and 5. Sensitivity to the size of the perturbation and the importance of the geographical distribution of emissions are investigated in sections 6 and 7. A description of the radiation code and the radiative impacts of the composition changes are presented in section 8. We conclude with a discussion of our findings.

## 2. Model Configuration

[6] The 3D chemistry transport model p-TOMCAT [O'Connor et al., 2005; Cook et al., 2007] is an updated and parallelized version of the earlier TOMCAT model [Law et al., 1998, 2000; Savage et al., 2004]. It includes a gas-phase methane-oxidation scheme with simplified NMHC treatment (ethane, propane) on 35 hybrid-pressure levels from the surface to 10 hPa, with a vertical resolution of approximately 700 m in the upper troposphere and lower stratosphere (UTLS) region. In order to achieve the number of integrations required for this study we have chosen a horizontal grid resolution of  $5.6 \times 5.6$  degrees which adequately represents the global distribution of aircraft emissions. At the upper boundary  $\text{O}_3$ ,  $\text{CH}_4$  and  $\text{NO}_y$  are prescribed with climatological values from the Cambridge 2D-Model [Law and Pyle, 1993]. Photolysis rates are calculated off-line with the Cambridge 2D model. A recent validation of TOMCAT with airborne observations together with an intercomparison of its results with those from other models is published by Brunner et al. [2003, 2005]. Therein

it is shown that the model is capable of reproducing contemporary atmospheric background conditions and the results are within the range calculated by other atmospheric models. For the experiments in this study the model was forced by ECMWF operational analyses for 2001 and 2002. The year 2001 served as a spin-up period and only the results from 2002 are shown in this study.

[7] The p-TOMCAT model does not consider heterogeneous and halogen chemistry in the stratosphere and its upper boundary is located at 10 hPa (32 km). This allows only a limited representation of stratospheric processes. For this purpose a subset of the experiments was also carried out using the SLIMCAT chemistry transport model [Chipperfield, 1999] to investigate the impact of aircraft emissions specifically in the stratosphere. The SLIMCAT model is forced by UKMO analyses and incorporates a stratospheric chemistry scheme on 18 isentropic levels between 335 K and 2700 K (10–55 km). A spin-up integration of 6 perpetual years of 2001 meteorology prior to one year of 2002 meteorology ensures the appropriate representation of transport timescales within the stratosphere.

[8] The lifetime of methane with respect to chemical removal by hydroxyl radicals (OH) in this version of p-TOMCAT is determined as 13.5 years when aircraft  $\text{NO}_x$  emissions are included. This value is at the upper limit of the model range presented in IPCC [2001] and  $\sim 40\%$  above the mean value of 9.6 years. In our sensitivity studies we focus however on the fractional lifetime change caused by perturbations to  $\text{NO}_x$  emissions and therefore results are relatively insensitive to the base lifetime. The inclusion of stratospheric and soil sinks which are assumed to be  $40 \text{ Tg a}^{-1}$  and  $30 \text{ Tg a}^{-1}$ , respectively [IPCC, 2001], results in a global  $\text{CH}_4$  lifetime of 11.3 years. The inclusion of aircraft  $\text{NO}_x$  emissions to a model atmosphere without aircraft emissions leads to the increased formation of OH which increases the oxidizing capacity of the troposphere and reduces the lifetime of  $\text{CH}_4$ . This in turn enhances the initial OH perturbation through a positive feedback [Prather, 1994]. The steady state  $\text{CH}_4$  concentration can be calculated, using the method shown by Fuglestvedt et al. [1999], without the need for integrating the model over several decades;  $\text{CH}_4$  concentrations are fixed in the model and we diagnose the initial change in OH due to altered  $\text{NO}_x$  emissions. Steady state methane perturbations are then derived by applying a model-dependent feedback factor to the initial  $\text{CH}_4$  lifetime change with respect to OH. This feedback factor (the ratio of adjustment time to global lifetime, including stratospheric and soil sinks) is 1.3 for p-TOMCAT and was calculated from two reference experiments, the first of which had unaltered  $\text{CH}_4$  levels and the second had  $\text{CH}_4$  levels globally increased by 5%. The adjustment time of  $\text{CH}_4$  in p-TOMCAT is 30% longer than its global lifetime, at the lower limit of model ranges by IPCC [2001]. In this study a global annual mean 3-dimensional  $\text{CH}_4$  distribution obtained from an earlier long-term integration [Warwick et al., 2002] was used as a fixed boundary condition (global burden 4760 Tg  $\text{CH}_4$ ).

## 3. Experiment Description

[9] Experiments were designed to investigate the atmospheric response to perturbations in several key emission

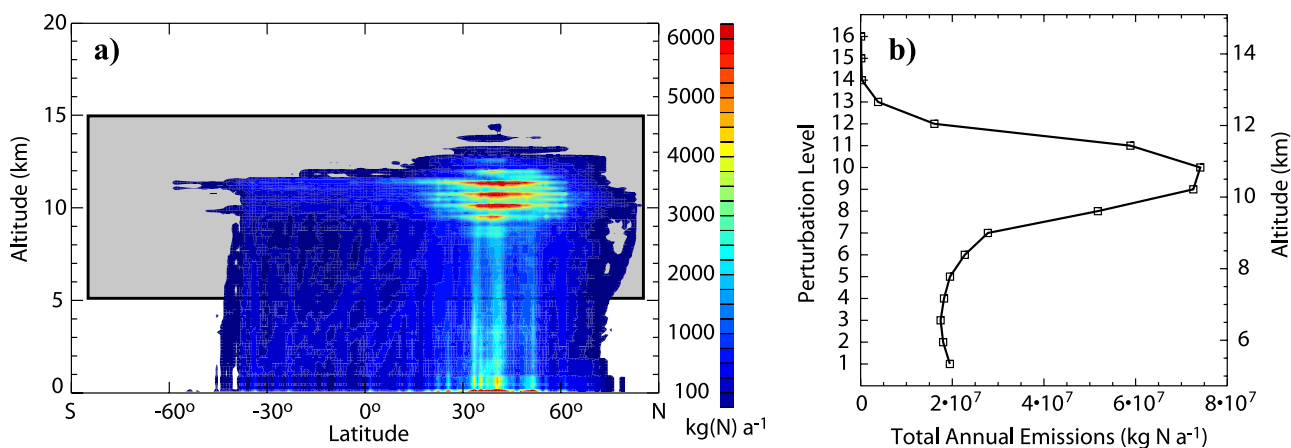


**Figure 1.** (a) AERO2k aircraft  $\text{NO}_2$  emissions for 2002 in  $\text{kg N a}^{-1}$  per  $1^\circ \times 1^\circ \times 500$  ft grid cell. At this vertical resolution the difference between flight levels with high and low air traffic is visible at cruise altitude in the northern midlatitudes. The altitude range of the perturbation levels is shown by the grey shaded box. (b) Total annual  $\text{NO}_x$  emissions on each of the 16 perturbation levels located inside the grey box of Figure 1a.

parameters: cruise altitude, size of the perturbation and the geographical distribution of emissions. They form a coherent set of sensitivity studies covering the complete altitude range where aircraft fly during cruise [IPCC, 1999] and where globally more than 60% of  $\text{NO}_x$  emissions from aircraft are released. The perturbations were applied to a reference emission distribution which was obtained from a global aircraft emission inventory. The aircraft  $\text{NO}_2$  emission data for 2002 from the European AERO2k Project [Eyers *et al.*, 2004] was used here as the reference with an annual total fuel usage of 176 Tg resulting in emissions of 0.68 Tg N. Figure 1a shows the zonally averaged annual total aircraft emissions from the AERO2k global inventory. The altitude range between 5 km and 15 km (16.5–48.5 kft), extending over the free troposphere and lower stratosphere, was divided into 16 equal cruise altitude bands of 610 m

(2000 ft) thickness, henceforth referred to as “perturbation levels” (Table 1). During each experiment, aircraft  $\text{NO}_x$  emissions were increased on a single perturbation level and the impact on  $\text{O}_3$  and  $\text{CH}_4$  abundances and the corresponding changes in radiative forcing were investigated. Figure 1b shows the annual total emissions on each perturbation level.

[10] In order to investigate sensitivities with respect to cruise altitude and magnitude of perturbation, emissions on perturbation levels 1–11 (5–11.7 km) were locally increased by 5% relative to the reference emissions. At selected levels, additional experiments with increases of 10% and 20% were carried out. The magnitude and location of these perturbations might represent the introduction of a new additional aircraft type to the existing global fleet. By comparing the atmospheric impact, normalized by the size

**Table 1.** Perturbation Levels and Normalized Radiative Forcing Due to Change in  $\text{O}_3$  and  $\text{CH}_4$ , as a Function of Altitude at Which the  $\text{NO}_x$  Emissions are Perturbed<sup>a</sup>

Perturbation Level	Altitude, km <sup>b</sup>	Emission Scaling	$\text{O}_3$ Radiative Forcing, $\text{mWm}^{-2}/\text{Tg N a}^{-1}$	$\text{CH}_4$ Radiative Forcing, $\text{mWm}^{-2}/\text{Tg N a}^{-1}$
16	14.2–14.8	VG: 2838%, CG: 5% of level 11	174.6	–39.0
15	13.6–14.2	VG: 2185%, CG: 5% of level 11	90.1	–29.5
14	13.0–13.6	VG: 1060%, CG: 5% of level 11	59.6	–27.8
13	12.4–13.0	VG: 77.2%, CG: 5% of level 11	76.6	–29.8
12	11.7–12.4	VG: 18.3%, CG: 5% of level 11	64.1	–26.9
11	11.1–11.7	5%, 10%, 20%	88.0	–41.1
10	10.5–11.1	5%	77.3	–38.5
9	9.9–10.5	5%	61.1	–33.1
8	9.3–9.9	5%, 10%, 20%	54.5	–31.9
7	8.7–9.3	5%	50.3	–31.5
6	8.1–8.7	5%	43.7	–31.6
5	7.5–8.1	5%, 10%, 20%	38.5	–32.1
4	6.9–7.5	5%	38.4	–32.7
3	6.3–6.9	5%	33.5	–32.5
2	5.6–6.3	5%, 10%, 20%	30.1	–31.3
1	5.0–5.6	5%	25.4	–29.4

<sup>a</sup>The methane-induced  $\text{O}_3$  forcing can be obtained by multiplying the methane forcing by 0.59.

<sup>b</sup>Perturbation levels (PL) have a vertical thickness of 2000 feet. The altitude offset was chosen such that the PL boundaries are located between flight levels used by air traffic management [cf. Eyers *et al.*, 2004].

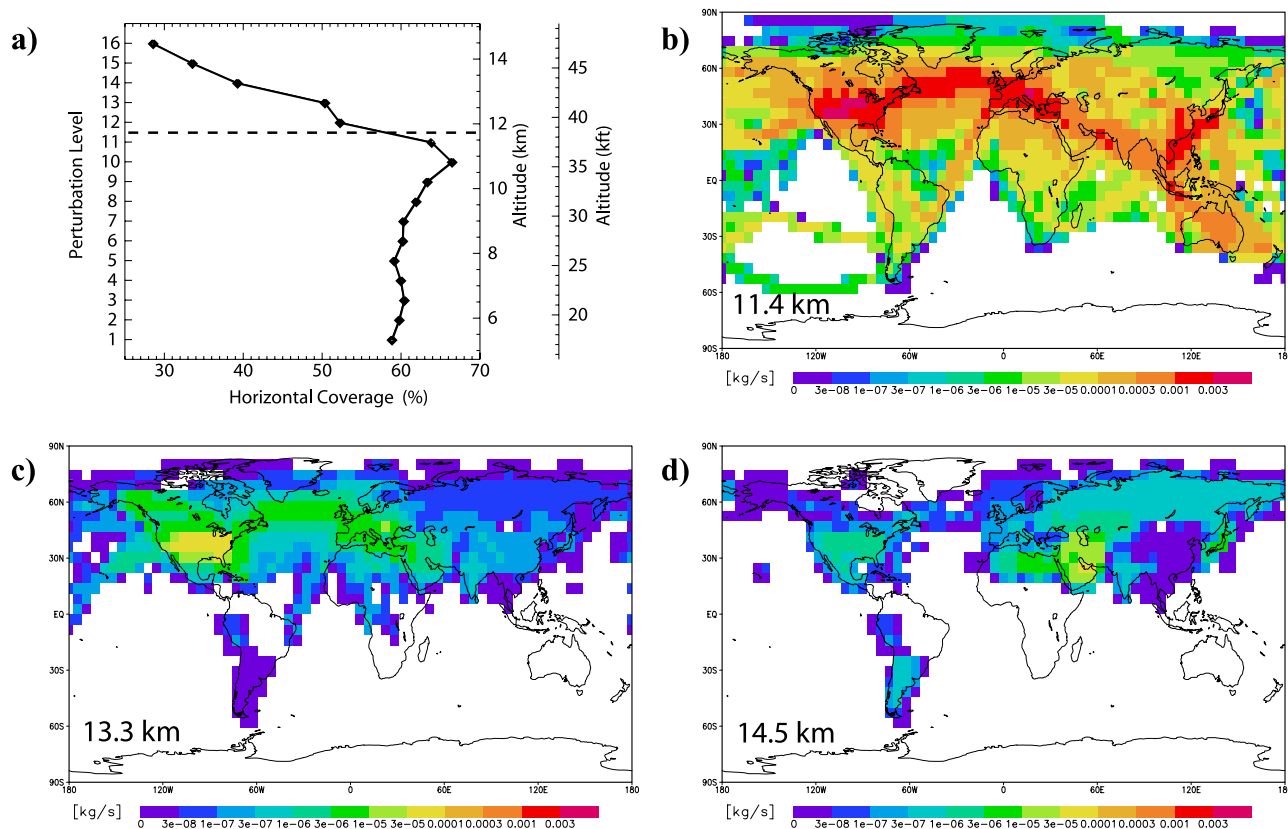


**Figure 2.** (a) Global coverage of emission perturbations in percent of the horizontal model grid for each perturbation level. (b)–(d) Geographical distribution of NO<sub>x</sub> emission perturbations for levels 11, 14, and 16.

of the emission increase, it is possible to identify cruise altitude bands where the atmospheric response is particularly sensitive to emission perturbations. In addition it is possible to study the relationship between the atmospheric response and emission increases of varying magnitude. Above level 11 (11.4 km) the total emitted NO<sub>x</sub> in the reference emission distribution declines rapidly such that an increase of 20% or less is too small to produce a reliable response in the model calculations after normalization.

[11] In further experiments the atmospheric sensitivity to changes in the geographical distribution of aircraft emissions is investigated at different perturbation levels. Figure 2a shows the geographical distribution of aircraft emissions for each perturbation level expressed as a percentage of the global horizontal model domain. Aircraft emissions cover approximately 60% of the globe on perturbation levels 1–11 with a maximum coverage at level 10. This geographical coverage becomes significantly smaller at altitudes above level 11 (see Figure 1). Figures 2b–2d show the geographical distributions of the emission perturbations on levels 11, 14, and 16 as examples and illustrates that not only do total emissions decrease, but the geographical distribution of the emissions becomes more limited. In order to address the concern that any apparent change in the impact of emissions as a function of altitude could in reality be due to the change in sensitivity to both horizontal and vertical distribution of emissions, two types of geographical perturbation experiment were carried out for levels 12–16 (11.7–14.8 km). In

the first experiment type, referred to as “CG” (Constant Geographical distribution), the additional emissions created by a 5% local increase on level 11 were vertically shifted to perturbation levels 12–16 while maintaining the geographical distribution and magnitude exhibited on level 11. In the second experiment type, referred to as “VG” (Varying Geographical distribution), the emissions on levels 12–16 were scaled such that the total global emission increase on each level was equal in size to the emission increase from a 5% scaling on level 11. For each level 12–16 an individual scaling factor was used in VG, but the geographical coverage of the emissions remained unchanged from that in the reference distribution. It is important to note that, in consequence, the size of the emission change in both experiments CG and VG is equal in mass for each perturbation level, but that the geographical coverage varies.

#### 4. Effects of Aircraft Emissions

[12] The inclusion of AERO2k aircraft NO<sub>x</sub> emissions relative to a case without aviation emissions leads to a net increase in ozone by enhancing ozone production through increased chemical cycling of NO<sub>x</sub> both in the troposphere and lower stratosphere. Some ozone loss occurs at high altitudes due to catalytic destruction. Figure 3 shows the changes in ozone calculated by p-TOMCAT and SLIMCAT. Ozone mixing ratios increase by approximately 6–9 ppbv in the UTLS region, where aircraft emissions have the largest

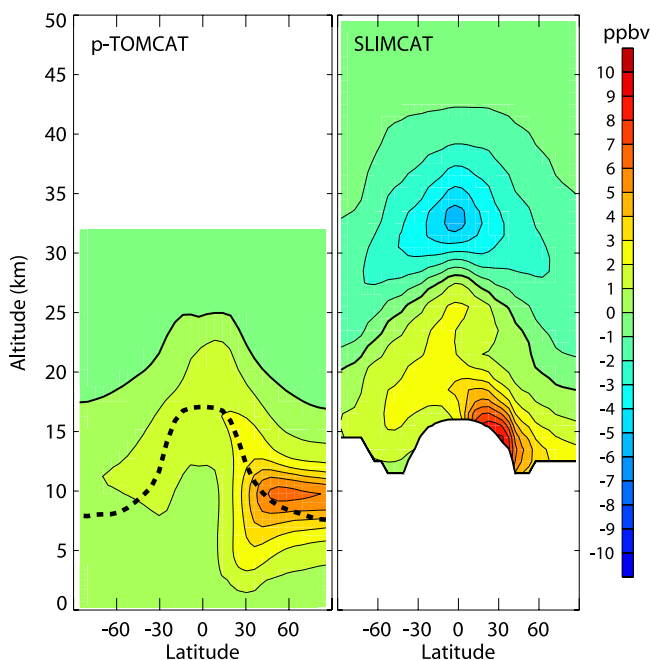


**Figure 3.** Zonal and annual mean  $O_3$  changes as calculated by p-TOMCAT (after 2 years) and SLIMCAT (after 7 years). The dashed line indicates the location of the tropopause (2 PVU surface). SLIMCAT data are shown above the tropopause and above the 335 K isentropic surface only. Changes in mixing ratios are shown with respect to a background atmosphere without aircraft emissions.

impact. Transport of ozone to lower altitudes and latitudes leads to increased ozone levels throughout the troposphere with the largest impact in the northern hemisphere. *Rogers et al.* [2002] have shown that the SLIMCAT model exhibits an efficient uplift of subsonic aircraft emissions within the “tropical pipe”, which conversely results in an efficient downward transport in the extra-tropics. This leads to the near-tropopause maximum  $O_3$  increase from aircraft  $NO_x$  to be located in SLIMCAT at lower latitudes than in the p-TOMCAT model, and to the vertical transport of aircraft  $NO_x$  to altitudes above 30 km. Above  $\sim 25$  km altitude aircraft  $NO_x$  emissions contribute to catalytic  $O_3$  destruction and result in a small decrease (5 ppbv) in stratospheric ozone. In total, aircraft  $NO_x$  leads to a global  $O_3$  burden increase of 8.8 Tg. These findings are in reasonable agreement with those from IPCC [1999], *Grewe et al.* [2002b] and with earlier TOMCAT results [*Köhler et al.*, 2004]. They exceed slightly however the range of model results from the European TRADEOFF Project [*Isaksen*, 2003] which peak at 3–6 ppbv in the UTLS in July. *Gauss et al.* [2006a] report an annual mean  $O_3$  increase in the upper troposphere of up to 4 ppbv. There are many possible reasons for the inter-model differences, including the emissions inventory and model formulations such as the chemistry schemes, convective transport schemes, and wet deposition schemes employed. One contributor to the difference is that the present work does not include the effect of plume processing of aircraft  $NO_x$  emissions which have been estimated to reduce the effective emissions to the

model gridboxes by up to 30% (M. Gauss, personal communication, 2007).

[13] Ozone loss in the middle stratosphere is more pronounced in the SLIMCAT results, where, during the longer spin-up period,  $NO_x$  from aircraft emissions is transported higher into the middle stratosphere. Both models show good agreement in the meridional distribution of the “crossover point” between the domains with ozone increase and decrease ( $\sim 22$  km, see Figure 3). We are therefore confident that the results from the p-TOMCAT model are representative for the troposphere and the lower stratosphere. At altitudes above the crossover point p-TOMCAT results become less representative due to the proximity of the upper boundary (32 km), the duration of the integration, and the absence of a complete stratospheric chemistry.

[14] The partial ozone column changes below and above the crossover point are given in Table 2. The ozone column increases in the global and annual average due to aircraft emissions by 0.81 DU in p-TOMCAT and 0.83 DU in SLIMCAT with a strong bias to the northern hemisphere where more aircraft emissions are released. Figure 9 shows the seasonal and meridional  $O_3$  column change in p-TOMCAT. From June to November the monthly AERO2k emission rates are approximately 10% larger than during the other months, with a maximum in August which contributes to the autumn peak in the  $O_3$  column change. These ozone column changes significantly exceed those shown by *Stordal et al.* [2006]. In p-TOMCAT the reduction of the ozone column above the crossover point is substantially smaller than calculated by SLIMCAT for reasons mentioned above. These results show that subsonic aircraft flying at present-day cruise altitudes affect ozone chemistry predominantly in the troposphere and lower stratosphere below 20 km altitude. The ozone impact above this altitude is relatively small given the large background ozone mixing ratios and, therefore, the fact that p-TOMCAT is restricted to a model domain below 10 hPa (32 km) is not a significant disadvantage in these studies.

[15] We diagnose the chemical production and loss of ozone by considering the reactions listed in Table 3; the results are shown in Figure 4. This approximation includes the dominant terms relevant for ozone production and loss in the troposphere and lower stratosphere. Note, for example, that catalytic ozone loss by  $NO_x$  is less important in this altitude range than catalytic  $HO_x$  cycles and therefore the  $NO_x$  reactions are omitted in this approximation. *Grewe et al.* [2002a] have investigated the effects of lower cruise altitudes on ozone production rates by using a linear

**Table 2.** Partial Ozone Columns in DU

	p-TOMCAT	SLIMCAT
Change above “crossover” <sup>a</sup>	−0.01	−0.19
Change below “crossover” <sup>b</sup>	0.82	1.02
Total $O_3$ Col.	0.81	0.83

<sup>a</sup>Partial  $O_3$  column calculated over the domain in the stratosphere above the cross-over point where ozone mixing ratios are decreased by aircraft  $NO_x$  emissions (approx. above 25 km).

<sup>b</sup>Partial  $O_3$  column calculated over the domain in the troposphere and lower stratosphere below the cross-over point where ozone mixing ratios are increased by aircraft  $NO_x$  emissions (between the surface and approx. 25 km). The cross-over point has been calculated for each gridbox column.

**Table 3.** Reactions for Ozone Production and Loss

P1	$\text{HO}_2 + \text{NO} \rightarrow \text{OH} + \text{NO}_2$
P2	$\text{CH}_3\text{OO} + \text{NO} \rightarrow \text{HO}_2 + \text{HCHO} + \text{NO}_2$
P3	$\text{C}_2\text{H}_5\text{OO} + \text{NO} \rightarrow \text{CH}_3\text{CHO} + \text{HO}_2 + \text{NO}_2$
P4	$\text{CH}_3\text{CO}_3 + \text{NO} \rightarrow \text{CH}_3\text{OO} + \text{CO}_2 + \text{NO}_2$
P5	$n\text{-C}_3\text{H}_7\text{OO} + \text{NO} \rightarrow \text{C}_2\text{H}_5\text{CHO} + \text{HO}_2 + \text{NO}_2$
P6	$i\text{-C}_3\text{H}_7\text{OO} + \text{NO} \rightarrow (\text{CH}_3)_2\text{CO} + \text{HO}_2 + \text{NO}_2$
P7	$\text{C}_2\text{H}_5\text{CO}_3 + \text{NO} \rightarrow \text{C}_2\text{H}_5\text{OO} + \text{CO}_2 + \text{NO}_2$
P8	$\text{CH}_3\text{COCH}_2\text{OO} + \text{NO} \rightarrow \text{CH}_3\text{CO}_3 + \text{HCHO} + \text{NO}_2$
L1	$\text{HO}_2 + \text{O}_3 \rightarrow \text{OH} + \text{O}_2 + \text{O}_2$
L2	$\text{OH} + \text{O}_3 \rightarrow \text{HO}_2 + \text{O}_2$
L3	$\text{O}(^1\text{D}) + \text{H}_2\text{O} \rightarrow \text{OH} + \text{OH}$
L4	$\text{O}(^3\text{P}) + \text{O}_3 \rightarrow \text{O}_2 + \text{O}_2$

approach. In our study we diagnose reaction rate output directly from p-TOMCAT's chemistry module.

[16] Figure 4 shows the change in  $\text{O}_3$  production and loss rates in July, as calculated by the p-TOMCAT model, due to the inclusion of aircraft emissions.  $\text{O}_3$  production peaks in the UTLS region where the largest amounts of  $\text{NO}_x$  are emitted (Box A on Figure 4). At the same time ozone loss through its reaction with  $\text{HO}_2$  is reduced due to an increased reaction of  $\text{HO}_2$  with  $\text{NO}$  (Box B), further enhancing net  $\text{O}_3$  production. A part of the additionally produced  $\text{O}_3$  is transported from the upper troposphere to lower altitudes where, in the presence of water vapor, it results in increased  $\text{HO}_x$  formation and therefore increased ozone loss (Box C). The increased  $\text{HO}_x$  levels in proximity to surface  $\text{NO}_x$  emission sources lead to  $\text{NO}_x$  being tied up more efficiently in reservoir species, such as  $\text{HNO}_3$ . We diagnose significant  $\text{HNO}_3$  increases in p-TOMCAT near the surface. This results in a reduction of the gross  $\text{O}_3$  production rate at low altitudes (Box D). This process has previously been

identified [e.g., *Stevenson et al.*, 2004] and is even stronger during winter (not shown). It should be noted that net ozone production due to aircraft  $\text{NO}_x$  emissions occurs only above 5 km altitude and exhibits a maximum at approximately 10 km where the largest amounts of  $\text{NO}_x$  are emitted by aviation. Therefore the increase in ozone below 5 km, seen in Figure 3, is due to advection of ozone from above, rather than by in situ production. Moreover, the transport of enhanced  $\text{O}_3$  due to aviation from above is responsible for the reduction in the net chemical  $\text{O}_3$  production below 5 km by enhancing the conversion from  $\text{NO}_x$  to  $\text{HNO}_3$ .

[17] Aircraft  $\text{NO}_x$  emissions increase OH levels primarily through additional production of  $\text{O}_3$  and additionally by shifting the  $\text{HO}_x$  balance in favor of OH [*Stevenson et al.*, 2004; *Berntsen et al.*, 2005]. The reaction of  $\text{NO}$  and  $\text{HO}_2$  occurs predominantly at cruise altitude whereas OH production via the photolysis of ozone in the presence of water vapor is particularly efficient in the lower troposphere at lower latitudes and involves transport of ozone into this region. This increase in tropospheric OH strengthens the principal loss reaction of OH with  $\text{CH}_4$  such that aircraft emissions are responsible for a reduction of the global methane lifetime by 3.0%. This result is in agreement with the range of values predicted by *IPCC* [1999] for the period between 1992 and 2015 after a feedback factor has been applied. *Stordal et al.* [2006] however report significantly smaller reductions in  $\text{CH}_4$  lifetime.

[18] The reduction in atmospheric methane has a secondary long-term impact on  $\text{O}_3$  which is smaller than the direct  $\text{O}_3$  impact by  $\text{NO}_x$ . The  $\text{O}_3$  increase diagnosed from a reference experiment with 5% more methane, which was used to establish the feedback factor, was linearly interpolated to determine the long-term  $\text{O}_3$  change due to a

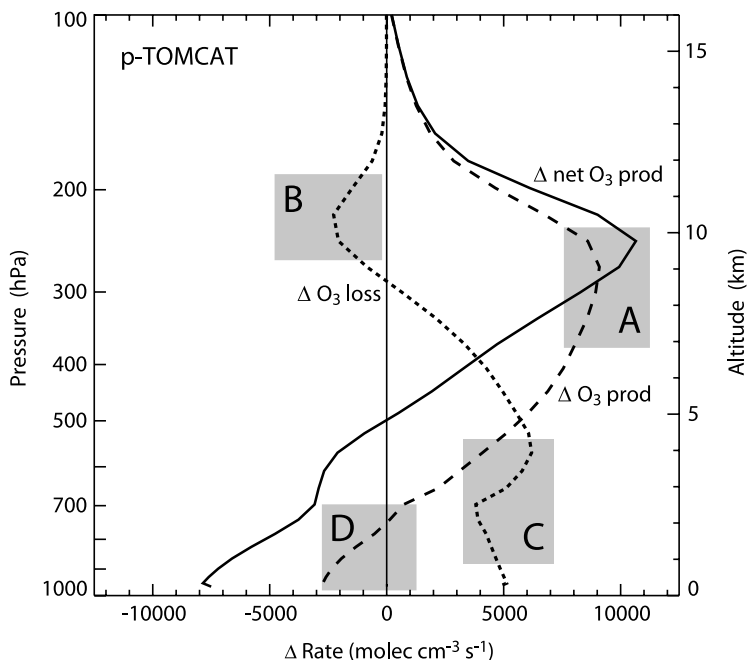


**Figure 4.** Change in gross  $\text{O}_3$  production (dashed line) and loss rates (dotted line) and net  $\text{O}_3$  production rate (solid line) due to the inclusion of AERO2k aircraft emissions in p-TOMCAT. The shaded boxes define regions of interest described in the text. Production and loss rates are calculated as zonal and meridional average for July 2002 using the reactions shown in Table 3.

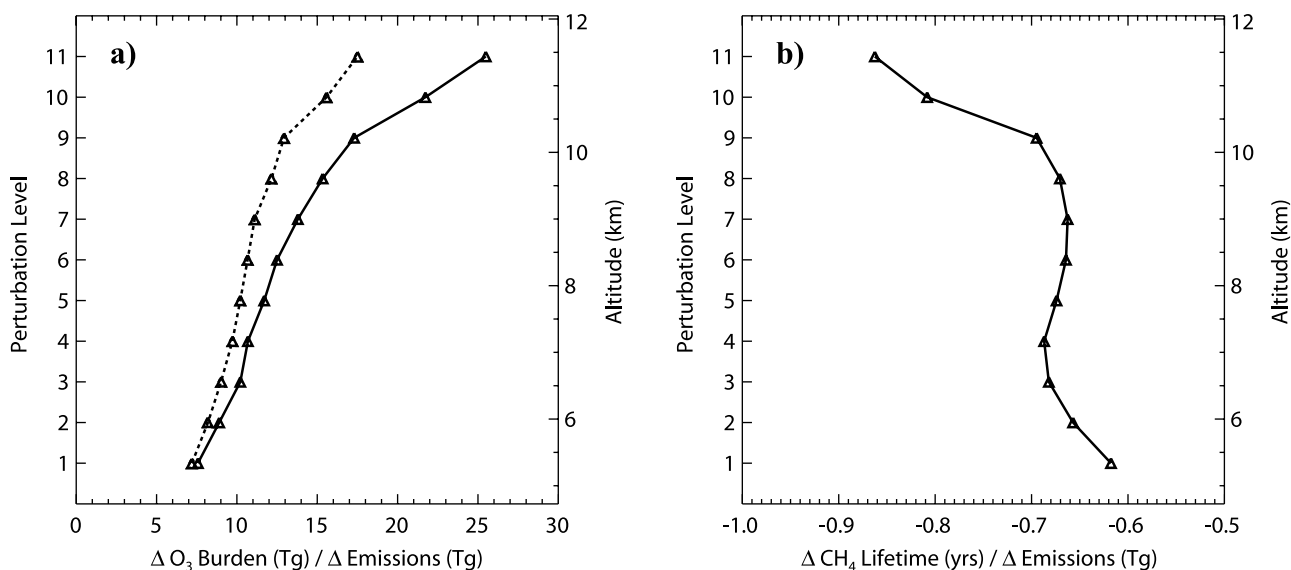


**Figure 5.** (a) Global (solid line) and tropospheric (dotted line) O<sub>3</sub> burden increase in p-TOMCAT due to a 5% NO<sub>x</sub> emission increase for each perturbation level, normalized by the global emission increase. The tropopause is defined as the 2 PVU surface. (b) CH<sub>4</sub> lifetime change normalized by the global emission increase.

reduction in the lifetime of CH<sub>4</sub> by 3%. The change in the CH<sub>4</sub> lifetime due to aircraft NO<sub>x</sub> reduces the global O<sub>3</sub> column by 0.27 DU and surface mixing ratios are reduced by approximately 0.1–0.2 ppbv. Despite being small, the fact that this constitutes a relatively long-lived perturbation means that it can make a significant contribution to the integrated climate effect of aviation emissions [e.g., Wild *et al.*, 2001; Stevenson *et al.*, 2004].

## 5. Effects of Emission Increases

[19] Perturbations to aircraft NO<sub>x</sub> emissions have an impact on atmospheric chemistry on both local and global scales. Ozone formation is affected both at the location of the emissions and further downwind following precursor transport. Ozone and NO<sub>x</sub> reservoir species have sufficiently long lifetimes to be transported over significant distances and as such influence the oxidizing capacity of the troposphere globally. The changes in the oxidizing capacity affect the lifetime of methane which is of the order of a decade, and therefore changes in methane are evenly distributed throughout the troposphere on a global scale. In order to consider the global atmospheric impacts of NO<sub>x</sub> as a function of the altitude of the emission perturbation, we focus in the following section on the changes to the global burdens of O<sub>3</sub> and CH<sub>4</sub>.

[20] In the altitude range 5–15 km, where in the following experiments emissions are perturbed, aircraft NO<sub>x</sub> emissions are found to result in net chemical ozone production (see previous section) and thus on all 16 perturbation levels an emission increase causes an increase of the global ozone burden. Emissions are increased by 5% on individual perturbation levels. Figure 5a shows the global ozone burden change normalized by the emission increase on each level for perturbation levels 1–11 (5–11.7 km). With increasing altitude the NO<sub>x</sub> balance is

shifted in favor of NO due to the temperature dependence of the reaction of NO with O<sub>3</sub> [Wild *et al.*, 1996; Jaeglé *et al.*, 1998b], reducing the conversion rate of NO<sub>x</sub> to HNO<sub>3</sub> and thus increasing the NO<sub>x</sub> lifetime with altitude. Liu *et al.* [1987] and Lin *et al.* [1988] have introduced the concept of the ozone production efficiency (OPE) as the ratio between production of ozone and loss of nitrogen oxides, which quantifies the efficiency of a NO<sub>x</sub> molecule in producing ozone during its lifetime. We calculate the OPE in January and July from the change in gross O<sub>3</sub> production due to an emission perturbation and from the associated change in loss of NO<sub>x</sub>. Our findings show that more than 97% of the NO<sub>x</sub> emission perturbation is converted into NO<sub>y</sub> and therefore we approximate the loss of NO<sub>x</sub> as being equal to the size of the emission perturbation. In both months we find that the OPE increases with altitude in the troposphere with a particularly sharp increase in the upper troposphere. Correspondingly Figure 5a shows that the impact on the total ozone burden increases with the altitude of the applied emission change. Emission changes at higher altitude are much more likely to be transported into the stratosphere and therefore at higher altitudes of the emission change a larger proportion of the stratospheric ozone burden is perturbed.

[21] The impact of NO<sub>x</sub> emissions on the lifetime of methane and its dependence on altitude are shown in Figure 5b. The photolysis of additional ozone, produced from aircraft NO<sub>x</sub> emissions, in the presence of water vapor leads to the formation of OH and results in a reduction of the CH<sub>4</sub> lifetime. This process is particularly efficient when ozone production is large, and when ozone is transported to lower altitudes and latitudes where ambient H<sub>2</sub>O concentrations and solar radiation levels are high. An increase in NO<sub>x</sub> emissions in regions with high ozone production efficiency, such as the upper troposphere, results in a larger reduction

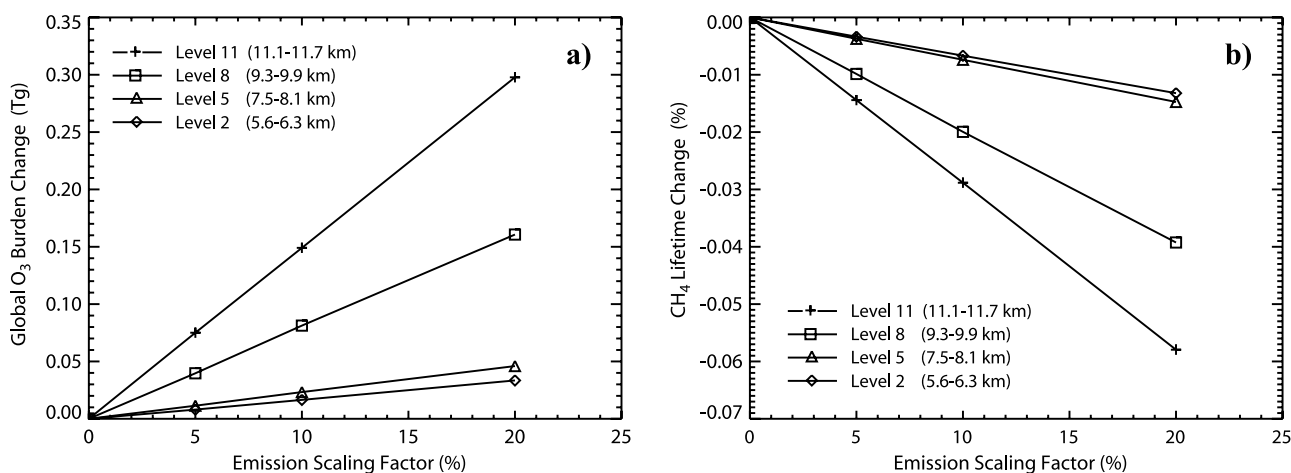


**Figure 6.** (a) Global changes in the ozone burden and (b) methane lifetime in p-TOMCAT due to scaling of aircraft emissions by 5%, 10% and 20% at perturbation levels 2, 5, 8, and 11, demonstrating the linear response.

in the CH<sub>4</sub> lifetime compared with lower altitudes. At 11.5 km altitude the lifetime decrease is 26% larger than at 10 km, while the impact is approximately constant below this altitude.

## 6. Linearity in the Chemical Response

[22] Having established the importance of the altitude dependence of NO<sub>x</sub> emissions, we now investigate the effects of increasing the size of the emission perturbation. This provides a test of the robustness of the earlier results by scaling the emissions with varying scaling factors. To do this the emissions are increased by 10% and 20% on one perturbation level at a time and results are compared with those from a 5% emission scaling. Because of the computational costs involved with the model integrations these experiments were only carried out on perturbation levels 2, 5, 8, and 11 (at 5.9, 7.8, 9.6, and 11.4 km, cf. Table 1) which span the vertical extent of the free troposphere.

[23] The results of emission scaling on the global ozone burden and the lifetime of methane are shown in Figure 6, and show that the response in ozone and methane is entirely linear for scaling factors up to 20% of the reference emissions. At higher altitudes the increase in the ozone burden and the reduction in the methane lifetime from the perturbation are stronger, in agreement with our findings from section 5. A further experiment with 200% emission scaling carried out on level 11 results in a global ozone burden increase that is only 5.3% smaller than the expected burden increase applying a linear scaling. This indicates that a linear atmospheric response may be valid even for emission scaling that significantly exceeds 20% at 11.4 km.

[24] In addition to the linearity in the total ozone burden we find that the vertical and horizontal distribution of the ozone perturbation is not altered by the emission scaling. Figure 7 shows the change in the vertical ozone profile (zonal mean) at 60°N caused by emission perturbations between 5% and 20% with respect to the reference experiment as calculated in p-TOMCAT and SLIMCAT. The change in the ozone profile at 20% is twice as large as for 10% changes and four times as large as for the 5% emission

increase. This linearity is found in p-TOMCAT below the crossover point and in SLIMCAT throughout the vertical model domain. The duration of the p-TOMCAT model integrations and the proximity of the upper boundary explain the non-linearities seen in the p-TOMCAT results above 18 km. The SLIMCAT results, which are not subject to these issues, show that the linearity in the O<sub>3</sub> change due to NO<sub>x</sub> perturbations is valid throughout the stratosphere. *Grewe et al.* [1999] and *Isaksen et al.* [2001] have shown by employing future aircraft emission scenarios that the atmospheric ozone response to a global increase in aircraft NO<sub>x</sub> emissions is approximately linear, even when changes to the atmospheric background conditions are taken into account. The findings from our study are consistent and show that the response to emission increases at individual cruise altitude bands is also linear.

[25] In addition to linear scaling of the emission size we investigate whether the atmospheric response to emissions at different cruise altitude bands is additive. Experiments are carried out with emissions scaled by 5% over two neighboring perturbation levels at once. We find that the sum of the ozone changes from individual perturbations applied accounts for more than 96% of the ozone change when the perturbation is applied to both levels simultaneously. These experiments were carried out for levels 2, 5, 8, and 11 and their respective lower neighboring level. The discrepancies in the vertical additivity of the ozone burdens vary in size and sign, but remain consistently below 4% of the burden change.

## 7. Effects of the Geographical Distribution of Emissions

[26] So far our results have shown that the atmospheric change due to small emission perturbations is both linear and nearly additive in response to a scaling of the reference emissions, provided the regional distribution of the emissions remains unchanged. In this section we investigate the atmospheric sensitivity to changes in the geographical distribution of the emissions, as performed in experiments CG and VG described in section 3.

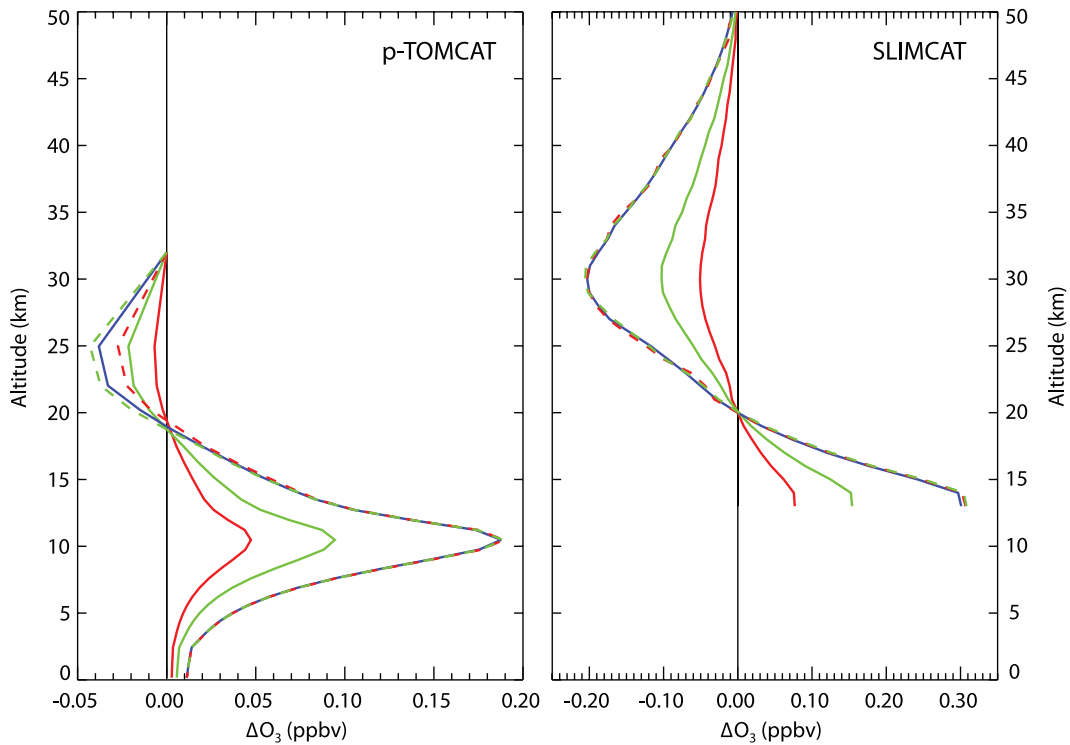


**Figure 7.** Change in the zonal mean ozone profile at 60°N due to emission scaling at 11.4 km altitude in p-TOMCAT (left) and SLIMCAT (right). The solid lines show the change due to 5% (red), 10% (green), and 20% (blue) emission scaling. The red and green dashed lines show the 5% and 10% scalings multiplied by factors of 4 and 2 respectively for comparison with the 20% scaling.

[27] Figure 8 shows the normalized changes in  $O_3$  burden and  $CH_4$  lifetime as calculated in the VG experiments on levels 12–16, where aircraft routing remains the same as for the reference emissions for the given level, and also those from the CG experiments where the

geographical flight distribution pattern of level 11 was used. It can be seen in Figure 8a that the  $O_3$  burden varies significantly between the individual perturbation levels in the VG experiments (squares). In the CG experiments the results show a continuous increase in the global ozone

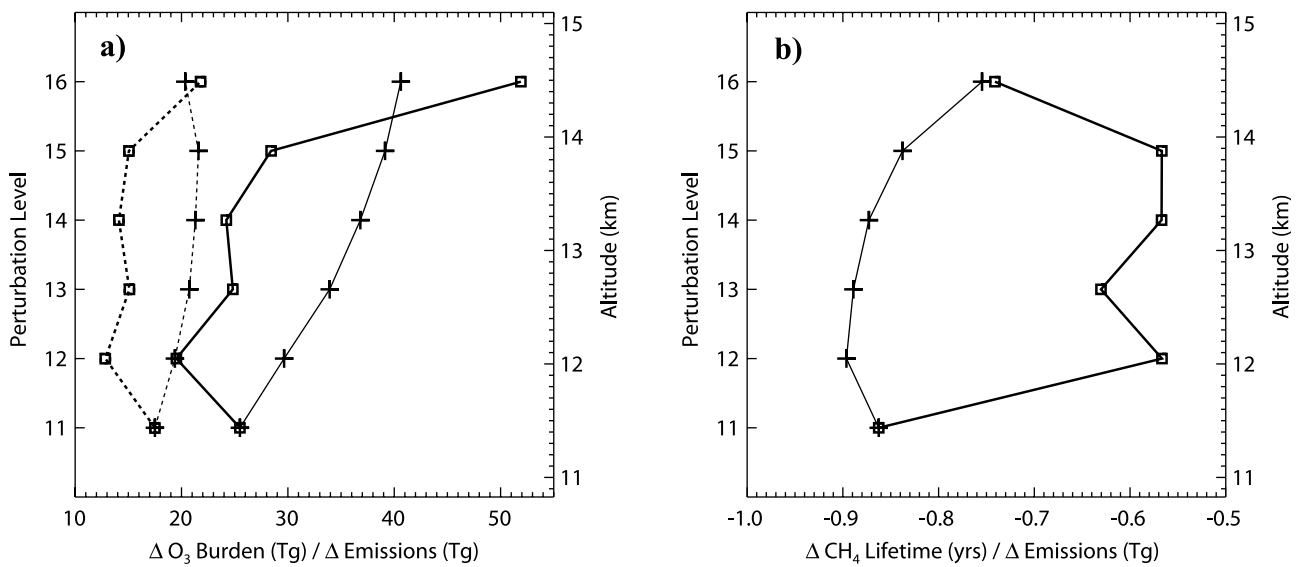


**Figure 8.** (a) Global (solid lines) and tropospheric (dotted lines) ozone burden change in p-TOMCAT normalized by the global emission increase. Lines with squares show the VG experiments, lines with crosses show the CG experiments. (b) As in (a) but for methane lifetime change. See section 3 for descriptions of the VG and CG experiments.

burden above level 11 (solid line with crosses). The difference between the lines with squares and crosses demonstrates the importance of the geographical distribution of the emissions. Figures 2b–2d show how the peak in emissions varies with latitude; the sharp increase in the  $O_3$  burden at level 16 in the VG experiment in Figure 8a is most likely a consequence of the emissions peak being located at lower latitudes in the Middle Eastern region. At level 14 the emissions peak is located over the U.S. and the North Atlantic Flight Corridor, at higher latitudes by comparison. In experiments CG the vertical shift of the emission perturbations from level 11 to higher altitudes results in an ozone response which is in general significantly stronger, both in the tropospheric and global burdens, than that caused by the emission distribution corresponding to actual flight routes on the same levels. For level 14 the ozone increase is 50% larger when emission distributions from level 11 are used compared to the original distribution, even though the total emitted  $NO_x$  is the same. The strong variability in the ozone response seen above level 11 in experiments VG is solely an artifact of the emission distribution and cannot be interpreted as a change in the sensitivity of atmospheric ozone with respect to  $NO_x$  emission increases. In fact, experiments CG show that with increasing altitude up to 14.5 km ozone production becomes increasingly sensitive to changes in  $NO_x$  emissions.

[28] For emission increases on levels 12–16 the majority of the perturbations are located within the stratosphere and with increasing altitude a larger proportion of the ozone increase also occurs within the stratosphere. The stability above the tropopause prevents the downward transport of ozone to lower altitudes where it contributes efficiently to OH production. Moreover  $H_2O$  mixing ratios in the lower stratosphere are much lower than in the lower troposphere resulting in less in situ OH production. Therefore the impact of  $NO_x$  emissions on the  $CH_4$  lifetime decreases with altitude above level 12 in the CG experiment when the emission perturbations and ozone changes are located within the stratosphere, as seen in Figure 8b. Again the regional redistribution of the emission perturbations results in a large impact on the  $CH_4$  lifetime, as shown by the difference between experiments CG and VG (crosses and squares).

[29] The extent to which changes in flight routing were applied in this study—by vertically shifting the emission perturbations of level 11—represents a significant but not entirely unrealistic alteration. The results show that the basis functions describing the linear and additive atmospheric response are dependent on the geographical distribution of the emissions and cannot be applied any longer when the geographical distribution has been altered significantly. This presents an important restriction to the formulation of a parametric relationship and merits further investigation. It is well established in models that the impact of  $NO_x$  surface emissions on ozone change is strongly dependent on the location of those emissions (see e.g., *Berntsen et al.* [2005], *Wild et al.* [2001] and references therein). Our study indicates that this also holds for emissions from aviation. Hence any change in the geographical distribution of emissions (for example due to growth in emerging markets in sub-tropical Asia) could lead to significant impacts on

ozone and methane levels, even if the overall global emissions remain constant.

## 8. Radiative Forcing

[30] Radiative forcings due to changes in ozone from aircraft  $NO_x$  emissions were calculated using a narrow band radiative transfer scheme, with 250 bands ( $10\text{ cm}^{-1}$ ) in the thermal infrared, 5 nm spectral resolution in the ultraviolet and 10 nm spectral resolution in the visible [*Forster and Shine*, 1997]; climatological cloud amounts were taken from *Rossow and Schiffer* [1999]. The monthly mean changes in ozone due to aviation for 2002 were used in the forcing calculations. Stratospheric temperature adjustment was included using the fixed dynamical heating approximation. Its impact was found to reduce the global annual mean instantaneous forcing due to air traffic by about  $-9\%$ , which is a smaller effect than found for purely tropospheric ozone cases [e.g., *Berntsen et al.*, 1997] probably because of the stratospheric component of the ozone forcing due to aviation  $NO_x$ . Because of the large number of perturbation experiments, the stratospheric adjustment was calculated only for four months for every second experiment. The same relative difference between instantaneous and adjusted forcings was found for these cases as for the case with reference aircraft emissions versus the case without aircraft emissions. Therefore the  $-9\%$  adjustment factor was applied to all the global annual means of instantaneous forcings.

[31] For the radiative forcing due to methane, a simpler approach is appropriate, in common with other similar studies [e.g., *Stordal et al.*, 2006]. Results from sophisticated radiative forcing codes have been shown to be well-represented by curve fits [*IPCC*, 2001]. For the relatively small methane perturbations found here, a linearization of this forcing around present-day methane amounts (1740 ppbv, and assuming background nitrous oxide concentrations of 319 ppbv, to account for spectral overlap) gives  $0.37\text{ mWm}^{-2}\text{ ppbv}^{-1}$ .

[32] Note that we use radiative forcing as a way of quantifying and comparing the climate effect of aviation  $NO_x$  emissions, but two important caveats are necessary. First, there has been much recent work comparing the efficacy of different forcings; the efficacy gives the ratio of global-mean surface temperature change for a  $1\text{ Wm}^{-2}$  forcing due to a given forcing mechanism compared to the surface temperature change for a  $1\text{ Wm}^{-2}$  forcing due to a change in carbon dioxide. As shown by *Ponater et al.* [2006], efficacies due to aviation-induced forcings can depart significantly from unity; for their model, *Ponater et al.* [2006] find values of 1.37 for ozone and 1.18 for methane forcings. We do not apply these efficacies here as it is necessary to establish the degree of model dependence of these results, but they are nevertheless indicative of a possible significant effect. The second caveat, which is to some extent related to the efficacy issue, is that caution must be exercised in comparing the apparently offsetting effects of the positive ozone and negative methane forcings, as the former is concentrated in the northern hemisphere, while the latter is global in extent [e.g., *IPCC*, 1999].

[33] The cloudy-sky global-mean adjusted radiative forcing, due to the  $NO_x$ -induced ozone changes from the

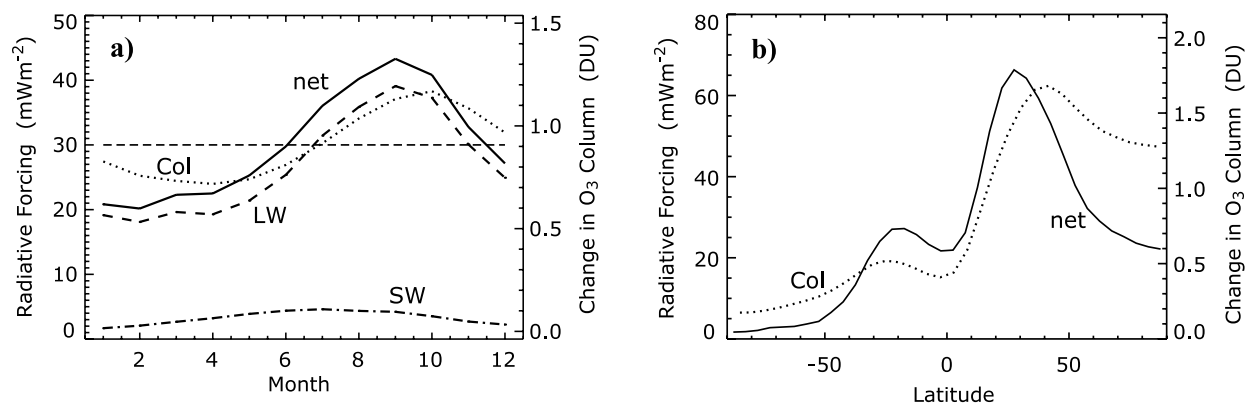


**Figure 9.** (a) Seasonal variation in global O<sub>3</sub> column in p-TOMCAT and global mean adjusted radiative forcing at the tropopause due to O<sub>3</sub> changes from inclusion of aircraft emissions, for longwave, shortwave and net forcings. (b) Zonal and annual mean changes in O<sub>3</sub> column and associated radiative forcing.

AERO2k emissions derived using the p-TOMCAT model, was found to be 30 mWm<sup>-2</sup> relative to the case with no aviation emissions. This value is consistent with the IPCC [1999] value of 23 mWm<sup>-2</sup>, which was derived for NO<sub>x</sub> emissions of 0.58 Tg N a<sup>-1</sup>; simple linear scaling to the AERO2k value of 0.68 Tg N a<sup>-1</sup> would yield a forcing of 27 mWm<sup>-2</sup>.

[34] Our value is somewhat greater than the mid-range value of 22 mWm<sup>-2</sup> given by Sausen *et al.* [2005]; they report, without details, a range of 12–28 mWm<sup>-2</sup> using the TRADEOFF inventory for the year 2000 and a range of chemistry transport models and radiation codes. Stordal *et al.* [2006] report a reduced range of 11 to 16 mWm<sup>-2</sup> for a subset of the models used by Sausen *et al.* [2005] and for emissions of 0.59 Tg N a<sup>-1</sup>. It is also known that the radiation code used by Stordal *et al.* [2006] yields forcings about 11% lower than the code used here [Gauss *et al.*, 2006b]. However, adjusting for this difference and the difference in NO<sub>x</sub> emissions would alter the Stordal *et al.* [2006] range to 14 to 20 mWm<sup>-2</sup>, still smaller than our result. As discussed in section 4, p-TOMCAT yields significantly larger changes in ozone than the models used for forcing calculations in the Stordal *et al.* [2006] study and this accounts for most of the difference in the ozone forcing. By contrast, Ponater *et al.* [2007] report a forcing of 60 mWm<sup>-2</sup> for the DLR 2015 emissions scenario [Grewe *et al.*, 2002b] which corresponds to 1.18 Tg N a<sup>-1</sup>; simple linear scaling would yield a forcing of 35 mWm<sup>-2</sup> using the AERO2k NO<sub>x</sub> emissions.

[35] The monthly and global-mean forcing is shown in Figure 9a and shows a strong peak in forcing in September to November, consistent with the peak change in ozone. Figure 9a also shows, as expected, the dominance of the longwave forcing over the shortwave forcing. Figure 9b shows the annual and zonal-mean adjusted forcings to allow comparison with other work [e.g., IPCC, 1999; Stordal *et al.*, 2006] and emphasizes the northern hemisphere dominance of this forcing for the current aviation fleet. The marked secondary peak at 20°S in Figure 9b is entirely absent by Hauglustaine *et al.* [1994]. There is a smaller secondary peak in the work of IPCC [1999] (see their Figures 5–8) and there are hints of a small peak in

the three models reported by Stordal *et al.* [2006]. As shown by Stordal *et al.* [2006], the TOMCAT model (the predecessor to the model used here) has a heightened southern hemisphere ozone response to aviation emissions, and a more marked secondary peak, than the other models in that study. Figure 10 shows the annual-mean geographical distribution of total ozone change and forcing. It shows that the peak in forcing is displaced much more toward the equator than the emissions themselves (cf. Figure 3). This is partially because of the location of the ozone changes (Figure 10a), but also because a given change in tropospheric ozone is much more effective at causing radiative forcing at lower latitudes particularly over warm, relatively high albedo surfaces such as deserts [e.g., Bernsten *et al.*, 1997].

[36] The impact of the NO<sub>x</sub> perturbation experiments (section 5) on radiative forcing are shown both for a 5% change in NO<sub>x</sub> emissions in Figure 11a and normalized to the NO<sub>x</sub> emissions in Figure 11b. The 5% plot shows a strong peak at 10.5 km, coincident with the peak in NO<sub>x</sub> emissions (cf. Figure 1). The normalized plot shows a general increase in forcing per Tg N a<sup>-1</sup> emitted with altitude – the structure in the 11–13 km region is because these calculations use the VG experiments (cf. Figure 8), so part of the variation is due to the change in the geographical distribution of the fleet with altitude. The dominant driver of the vertical variation between 11 and 15 km altitude is that, as shown in Figure 5, a given emission of NO<sub>x</sub> leads to a greater ozone increase at higher altitudes. Although a given change in ozone is generally more important for radiative forcing if it is located near the tropopause, this is a secondary effect in driving the vertical variation of the forcing as a function of the altitude of perturbation. Advection by the circulation means that the perturbation to ozone is not strongly constrained to the altitude at which NO<sub>x</sub> is perturbed. We find that the forcing per change in column ozone burden varies by only 10% with height of NO<sub>x</sub> perturbation; the peak effect is for perturbation level 7 (about 9 km).

[37] The radiative forcing due to the methane lifetime decrease of 3.0% (section 4) is about −19 mWm<sup>-2</sup>, again very similar to the IPCC [1999] value when scaled for

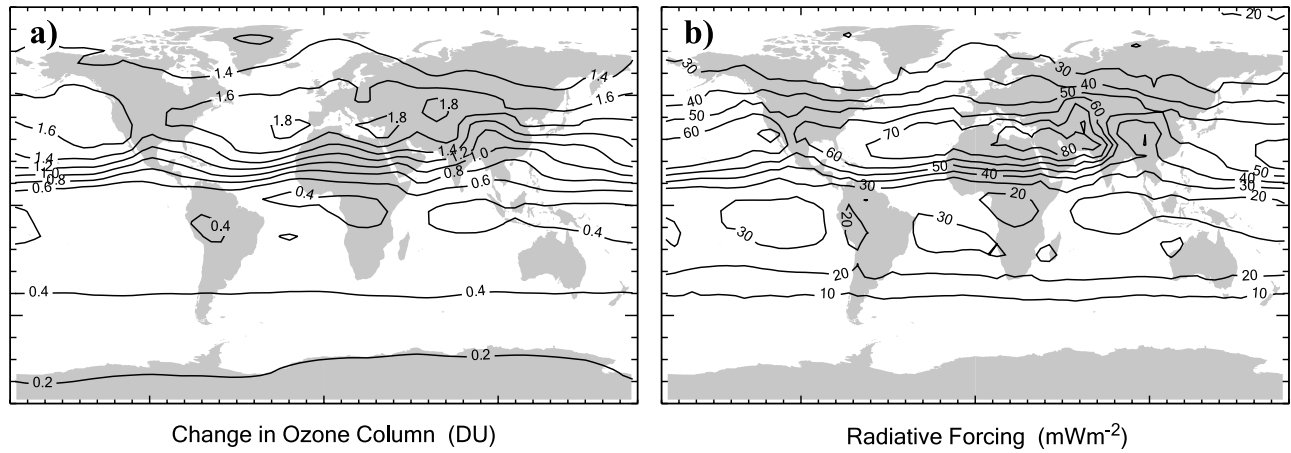


**Figure 10.** Geographical distribution of (a) annual mean O<sub>3</sub> column changes (in DU) from inclusion of aircraft emissions in p-TOMCAT and (b) annual mean radiative forcing due to ozone changes (in mWm<sup>-2</sup>).

changes in emissions, but somewhat more negative than the mid-range Sausen *et al.* [2005] value of  $-10.4 \text{ mWm}^{-2}$ . Note however that, insofar as a net forcing can be produced from the sum of the ozone and methane forcings, the net forcing from Sausen *et al.* [2005] of  $11.5 \text{ mWm}^{-2}$ , is very similar to the  $11 \text{ mWm}^{-2}$  derived here.

[38] An estimate of the radiative impact of the methane change on ozone forcing can be made following the method

of Berntsen *et al.* [2005] (Appendix B), taking the IPCC [2001] multimodel mean value (see their Table 6.3) specific radiative forcing due to ozone change of  $42 \text{ mWm}^{-2} \text{ DU}^{-1}$ . As discussed in section 4, for p-TOMCAT the 3% decrease in methane leads to a column ozone decrease of 0.27 DU and hence this yields a forcing of  $-11 \text{ mWm}^{-2}$ ; using an average of a multimodel sensitivity of methane-induced

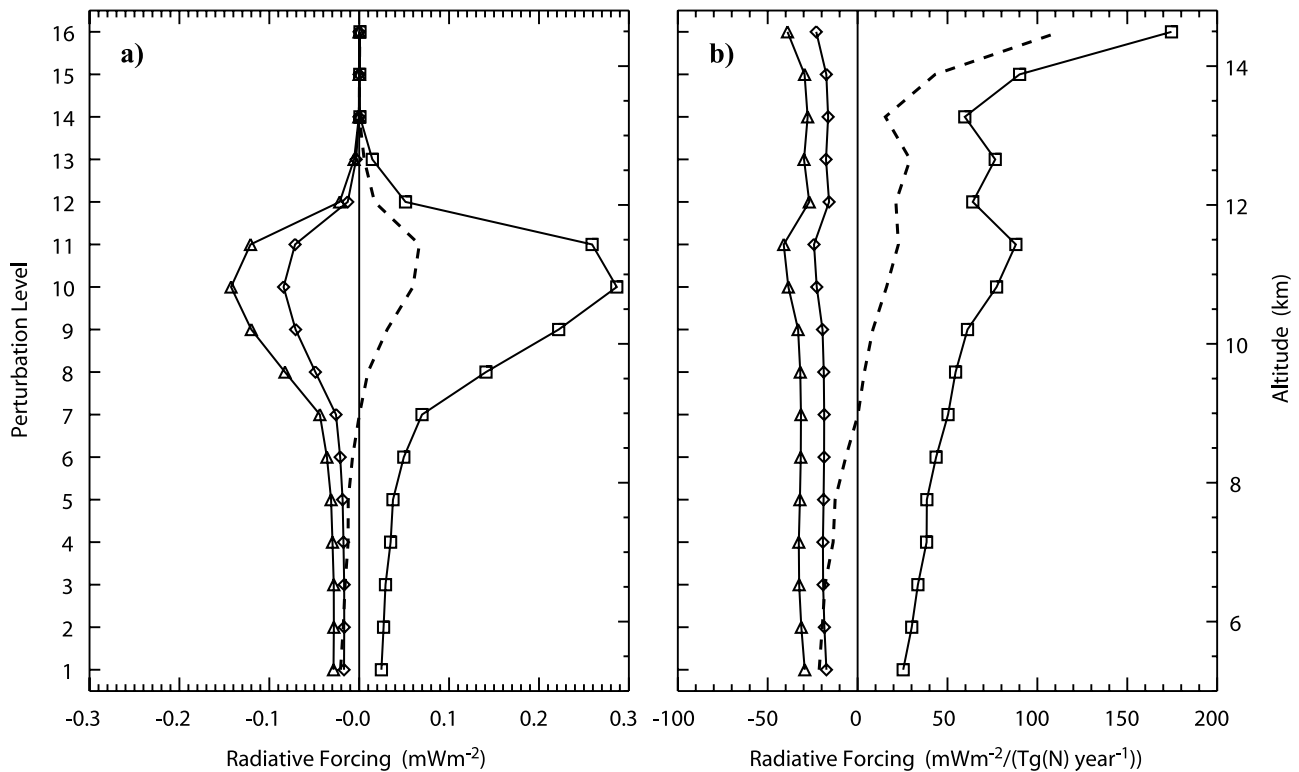


**Figure 11.** Radiative forcings due to changes in ozone (squares), methane (triangles) and methane-induced ozone change (diamonds) as a function of the altitude of a NO<sub>x</sub> perturbation. The dashed lines represent the net forcing of all components. (a) Forcing in mWm<sup>-2</sup> due to a 5% perturbation in NO<sub>x</sub> emissions. (b) Forcing, normalized by the change in NO<sub>x</sub> emissions. Above level 11 the results were derived using the VG experiments and linearly scaled to 5%.

ozone changes (as used by *Berntsen et al.* [2005]), yields a slightly less negative forcing of  $-8 \text{ mWm}^{-2}$ .

[39] Hence the sum of the forcings due to short-lived ozone response, the methane response, and the methane-induced ozone is close to zero, in the global mean, emphasizing the importance of including the ozone response to methane change. Using the p-TOMCAT results, the ozone forcing due to the methane change is 0.59 times the methane forcing itself, for present-day methane concentrations. This ratio is also used to calculate the height variation of methane-induced ozone forcing.

[40] Figure 11 shows the methane radiative forcing as a function of height of the  $\text{NO}_x$  perturbation. As expected, this broadly follows the ozone forcing in shape, as both forcings are mostly dependent on the efficiency with which  $\text{NO}_x$  emissions change ozone amount. However, the normalized methane forcings per  $\text{Tg N a}^{-1}$  do not increase as rapidly as the ozone forcings in the stratosphere, because ozone changes in the stratosphere are less effective at changing tropospheric OH.

[41] Figure 11 also shows the simple estimate of the methane-induced ozone change, which is taken to be 0.59 times the methane forcing, and the sum of the three forcings. The normalized forcings (per  $\text{Tg N a}^{-1}$ ) for ozone and methane, as a function of the altitude of  $\text{NO}_x$  perturbation are also listed in Table 1.

## 9. Conclusions

[42] The impact of perturbations to a range of aircraft  $\text{NO}_x$  emission parameters on ozone and methane and the associated radiative forcing changes were investigated with two chemistry transport models and an off-line radiative transfer code. Initially the atmospheric impact of the unperturbed  $\text{NO}_x$  emissions from aviation in 2002 was calculated, using a new emission inventory and an updated version of the p-TOMCAT 3D chemistry transport model. Subsequently, the sensitivity toward changes in cruise altitude, the size of the emission perturbation and the geographical distribution of global emissions were investigated. Results from the SLIMCAT model reveal the long-term response at higher altitudes and demonstrate that the responses generated with p-TOMCAT in the critical upper troposphere/lower stratosphere region are reliable, and therefore provide evidence and additional support that p-TOMCAT is fit-for-purpose for these aircraft studies.

[43] Aircraft  $\text{NO}_x$  emissions increase the ozone mixing ratios in the troposphere and UTLS region, with a maximum increase of 6 ppbv in the zonal annual mean and a global increase in the  $\text{O}_3$  column of 0.81 DU. This is consistent with earlier results from TOMCAT and with results from IPCC [1999] and *Grewe et al.* [2002b] after linear scaling of their total aircraft emissions to AERO2k values. Results here however exceed those reported in TRADEOFF [*Isaksen*, 2003; *Gauss et al.*, 2006a; *Stordal et al.*, 2006]. The increase in ozone and the associated increase in the troposphere's oxidizing capacity has resulted in a reduction in the lifetime of methane by 3.0%. The ozone increase has led to an additional radiative forcing of  $30 \text{ mWm}^{-2}$ . This forcing is consistent with results from IPCC [1999], after the increase in  $\text{NO}_x$  emissions since 1992 is taken into account, and consistent with the top end of the range ( $28 \text{ mWm}^{-2}$ )

given by *Sausen et al.* [2005]. Clearly there remains significant uncertainty in the forcing, with most of this uncertainty being driven by uncertainty in the change in ozone from the aviation emissions. The methane decrease resulting from the ozone change is estimated to be  $-19 \text{ mWm}^{-2}$  and we make a simple estimate of the forcing due to methane-induced ozone forcing, which yields a value of  $-11 \text{ mWm}^{-2}$ . Hence the sum of the forcing from the three mechanisms considered here is, at least in the global mean, close to zero.

[44] The impact of aircraft  $\text{NO}_x$  emissions on ozone and methane depends significantly on cruise altitude, reflecting the increase in ozone production efficiency with altitude. An emission increase in the upper troposphere at 11 km leads to a 200% larger ozone increase and a 40% stronger reduction in methane lifetime per emitted mass of  $\text{NO}_x$  than an emission increase at 5 km altitude. Net chemical formation of ozone increased only above 5 km such that ozone increases below this altitude are due to downward transport of additional ozone being produced in higher regions. In the lower troposphere aircraft  $\text{NO}_x$  emissions lead to a reduction of the net ozone production, as the downward transport of aircraft-induced  $\text{O}_3$ , produced in the UTLS region, provides an additional local source of  $\text{HO}_x$  resulting in an increased loss of  $\text{O}_3$  and leading to nitrogen oxides at low altitudes being more efficiently tied up in nitric acid.

[45] The scaling of emissions at several cruise altitude bands has revealed that small changes in emissions (locally 5–20%) lead to a linear response in the  $\text{O}_3$ - $\text{NO}_x$ - $\text{CH}_4$  system and the associated radiative forcings. Moreover it was found that the effects from emission perturbations are approximately additive, such that the sum of the impacts from emission changes at different levels is near equal to the impact when emissions are perturbed simultaneously at all levels. Initial experiments with significantly larger scaling factors indicate that the linearity in the atmospheric response may be valid for scaling factors much larger than used in this study. This linear relationship can be used in future work to estimate the atmospheric impact of changes to a reference emission profile without the need to carry out chemistry transport model integrations, provided that the geographical distribution of the emissions remains unaltered. This restriction forms an important limitation to the applicability of a linear parameterization.

[46] Global aircraft emissions exhibit a maximum in terms of emitted mass and global coverage at 10–12 km altitude, above which they decrease rapidly with altitude. Correspondingly their impact on ozone and methane reaches a maximum at 10–12 km altitude. In spite of further increasing ozone production efficiency with altitude in the lower stratosphere, the variation of the geographical coverage of emissions results in a decrease in aircraft-induced ozone production and the impact on methane above 12 km. We have shown that a change to this coverage in the lower stratosphere, while maintaining the total amounts emitted, can lead to significant variations in the impact on ozone and methane. Changes applied to the geographical distribution of emissions result in a significant response in atmospheric ozone and methane that cannot be described by the linear base functions established earlier through emission scaling. This has important consequences for future air traffic growth, together with changes to flight routing as a result

of Air Traffic Control or operational procedures. In our study we investigated the impact of regional emission changes only at altitudes above 11.5 km where flight routing coverage changes substantially with altitude. Sensitivity to flight route distributions is likely to be found also at lower altitudes, although we expect the impact to be smaller as the total geographical coverage of emissions exhibits less variability at lower altitudes.

[47] **Acknowledgments.** This study was funded by Airbus and the U.K. Department of Trade and Industry. The authors would therefore like to express their particular gratitude to C. J. Hume and P. J. Newton for their support. We thank three reviewers for their constructive comments. We also would like to thank members of the EU FP5 AERO2k Project (G4RD-CT-2000-00382) for providing access to the aircraft emission data.

## References

- Berntsen, T. K., I. S. A. Isaksen, G. Myhre, J. S. Fuglestedt, F. Stordal, T. Alsвик Larsen, R. S. Freckleton, and K. P. Shine (1997), Effects of anthropogenic emissions on tropospheric ozone and its radiative forcing, *J. Geophys. Res.*, 102(D23), 28,101–28,126.
- Berntsen, T. K., J. S. Fuglestedt, M. M. Joshi, K. P. Shine, N. Stuber, M. Ponater, R. Sausen, D. A. Hauglustaine, and L. Li (2005), Response of climate to regional emissions of ozone precursors: Sensitivities and warming potentials, *Tellus*, 57B(4), 283–304.
- Brasseur, G., G. T. Amanatidis, and G. Angeletti (Eds.) (1998), European scientific assessment of the atmospheric effects of aircraft emissions, *Atmos. Environ.*, 32(13), 2329–2418.
- Brunner, D., J. Staehelin, and D. Jeker (1998), Large-scale nitrogen oxide plumes in the tropopause region and implications for ozone, *Science*, 282(5392), 1305–1309.
- Brunner, D., et al. (2003), An evaluation of the performance of chemistry transport models by comparison with research aircraft observations, 1, Concepts and overall model performance, *Atmos. Chem. Phys.*, 3(5), 1609–1631.
- Brunner, D., et al. (2005), An evaluation of the performance of chemistry transport models by comparison with research aircraft observations, 2, Detailed comparison with two selected campaigns, *Atmos. Chem. Phys.*, 5(1), 107–129.
- Chameides, W. L., D. H. Stedman, R. R. Dickerson, D. W. Rusch, and R. J. Cicerone (1977), NO<sub>x</sub> production in lightning, *J. Atmos. Sci.*, 34(1), 143–149.
- Chipperfield, M. P. (1999), Multiannual simulations with a three-dimensional chemical transport model, *J. Geophys. Res.*, 104(D1), 1781–1805.
- Cook, P. A., et al. (2007), Forest fire plumes over the North Atlantic: p-TOMCAT model simulations with aircraft and satellite measurements from the ITOP/ICARTT campaign, *J. Geophys. Res.*, 112, D10S43, doi:10.1029/2006JD007563.
- Crutzen, P. (1973), A discussion of the chemistry of some minor constituents in the stratosphere and troposphere, *Pure Appl. Geophys.*, 106, 1385–1399.
- Eyers, C. J., P. Norman, J. Middel, M. Plohr, S. Michot, K. Atkinson, and R. Christou (2004), AERO2k global aviation emissions inventories for 2002 and 2025, Report number QinetiQ/04/01113, QinetiQ, Farnborough, Hampshire, U. K.
- Forster, P. M. de F., and K. P. Shine (1997), Radiative forcing and temperature trends from stratospheric ozone changes, *J. Geophys. Res.*, 102(D9), 10,841–10,857.
- Fuglestedt, J. S., T. K. Berntsen, I. S. A. Isaksen, H. Mao, X.-Z. Liang, and W.-C. Wang (1999), Climatic forcing of nitrogen oxides through changes in tropospheric ozone and methane; Global 3D model studies, *Atmos. Environ.*, 33(6), 961–977.
- Gauss, M., I. S. A. Isaksen, D. S. Lee, and O. A. Søvde (2006a), Impact of aircraft NO<sub>x</sub> emissions on the atmosphere - Tradeoffs to reduce the impact, *Atmos. Chem. Phys.*, 6(6), 1529–1548.
- Gauss, M., et al. (2006b), Radiative forcing since preindustrial times due to ozone change in the troposphere and lower stratosphere, *Atmos. Chem. Phys.*, 6(3), 575–599.
- Grewe, V., M. Dameris, R. Hein, I. Köhler, and R. Sausen (1999), Impact of future subsonic aircraft NO<sub>x</sub> emissions on the atmospheric composition, *Geophys. Res. Lett.*, 26(1), 47–50.
- Grewe, V., M. Dameris, C. Fichter, and D. S. Lee (2002a), Impact of aircraft NO<sub>x</sub> emissions, 2, Effects of lowering the flight altitude, *Meteorol. Z.*, 11(3), 197–205.
- Grewe, V., M. Dameris, C. Fichter, and R. Sausen (2002b), Impact of aircraft NO<sub>x</sub> emissions, 1, Interactively coupled climate-chemistry simulations and sensitivities to climate-chemistry feedback, lightning and model resolution, *Meteorol. Z.*, 11(3), 177–186.
- Hauglustaine, D. A., C. Granier, G. P. Brasseur, and G. Mégie (1994), Impact of present aircraft emissions of nitrogen oxides on tropospheric ozone and climate forcing, *Geophys. Res. Lett.*, 21(18), 2031–2034.
- IPCC (1999), *Aviation and the Global Atmosphere. A Special Report of Working Groups I and III of the Intergovernmental Panel on Climate Change*, edited by J. E. Penner et al., 373 pp., Cambridge Univ. Press, New York.
- IPCC (2001), *Climate Change 2001: The Scientific Basis. Contribution of Working Group I to the Third Assessment Report of the Intergovernmental Panel on Climate Change*, edited by J. T. Houghton et al., 881 pp., Cambridge Univ. Press, Cambridge, U.K.
- Isaksen, I. S. A. (Ed.) (2003), *Aircraft emissions: Contributions of various climate compounds to changes in composition and radiative forcing – Tradeoff to reduce atmospheric impact (TRADEOFF). Final report to the Commission of European Communities*, European Commission DG XII, Brussels, Contract No EVK2-CT-1999-0030.
- Isaksen, I. S. A., T. K. Berntsen, and W.-C. Wang (2001), NO<sub>x</sub> emissions from aircraft: Its impact on the global distribution of CH<sub>4</sub> and O<sub>3</sub> and on radiative forcing, *Terr. Atmos. Ocean. Sci.*, 12(1), 63–78.
- Jaeglé, L., D. J. Jacob, W. H. Brune, D. Tan, I. C. Faloona, A. J. Weinheimer, B. A. Ridley, T. L. Campos, and G. W. Sachse (1998a), Sources of HO<sub>x</sub> and production of ozone in the upper troposphere over the United States, *Geophys. Res. Lett.*, 25(10), 1709–1712.
- Jaeglé, L., D. J. Jacob, Y. Wang, A. J. Weinheimer, B. A. Ridley, T. L. Campos, G. W. Sachse, and D. E. Hagen (1998b), Sources and chemistry of NO<sub>x</sub> in the upper troposphere over the United States, *Geophys. Res. Lett.*, 25(10), 1705–1708.
- Köhler, M. O., H. L. Rogers, and J. A. Pyle (2004), Modelling the impact of subsonic aircraft emissions on ozone: Future changes and the impact of cruise altitude perturbations, in *Proceedings of a European Conference on Aviation, Atmosphere and Climate (AAC), Air Pollution Report* vol. 83, edited by R. Sausen et al., pp. 173–177, European Commission, Brussels.
- Lamarque, J.-F., G. P. Brasseur, P. G. Hess, and J.-F. Müller (1996), Three-dimensional study of the relative contributions of the different nitrogen sources in the troposphere, *J. Geophys. Res.*, 101(D17), 22,955–22,968.
- Law, K. S., and J. A. Pyle (1993), Modeling trace gas budgets in the troposphere, 1, Ozone and odd nitrogen, *J. Geophys. Res.*, 98(D10), 18,377–18,400.
- Law, K. S., P. H. Plantevin, D. E. Shallcross, H. L. Rogers, and J. A. Pyle (1998), Evaluation of modeled O<sub>3</sub> using measurements of ozone by Airbus in-service aircraft (MOZAIC) data, *J. Geophys. Res.*, 103(D19), 25,721–25,737.
- Law, K. S., et al. (2000), Comparison between global chemistry transport model results and measurement of ozone and water vapor by Airbus in-service aircraft (MOZAIC) data, *J. Geophys. Res.*, 105(D1), 1503–1525.
- Lin, X., M. Trainer, and S. C. Liu (1988), On the nonlinearity of the tropospheric ozone production, *J. Geophys. Res.*, 93(D12), 15,879–15,888.
- Liu, S. C., M. Trainer, F. C. Fehsenfeld, D. D. Parrish, E. J. Williams, D. W. Fahey, G. Hübler, and P. C. Murphy (1987), Ozone production in the rural troposphere and the implications for regional and global ozone distributions, *J. Geophys. Res.*, 92(D4), 4191–4207.
- O'Connor, F. M., G. D. Carver, N. H. Savage, J. A. Pyle, J. Methven, S. R. Arnold, K. Dewey, and J. Kent (2005), Comparison and visualisation of high-resolution transport modelling with aircraft measurements, *Atmos. Sci. Lett.*, 6(3), 164–170.
- Ponater, M., S. Pechtl, R. Sausen, U. Schumann, and G. Hüttig (2006), Potential of the cryoplane technology to reduce aircraft climate impact: A state-of-the-art assessment, *Atmos. Environ.*, 40(36), 6928–6944.
- Ponater, M., V. Grewe, R. Sausen, U. Schumann, S. Pechtl, E. Highwood, and N. Stuber (2007), Climate sensitivity of radiative impacts from transport systems, in *Proceedings of an International Conference on Transport, Atmosphere and Climate (TAC)*, edited by R. Sausen et al., pp. 190–195, European Commission, Brussels.
- Prather, M. J. (1994), Lifetimes and eigenstates in atmospheric chemistry, *Geophys. Res. Lett.*, 21(9), 801–804.
- Rädel, G., and K. P. Shine (2008), Radiative forcing by persistent contrails and its dependence on cruise altitudes, *J. Geophys. Res.*, 113, D07105, doi:10.1029/2007JD009117.
- Rogers, H., H. Teysse, G. Pitari, V. Grewe, P. van Velthoven, and J. Sundet (2002), Model intercomparison of the transport of aircraft-like emissions from sub- and supersonic aircraft, *Meteorol. Z.*, 11(3), 151–159.
- Rossov, W. B., and R. A. Schiffer (1999), ISCCP cloud data products, *Bull. Am. Meteorol. Soc.*, 72(1), 2–20.
- Sausen, R., et al. (2005), Aviation radiative forcing in 2000: An update on IPCC (1999), *Meteorol. Z.*, 14(4), 555–561.

- Savage, N. H., K. S. Law, J. A. Pyle, A. Richter, H. Nüß, and J. P. Burrows (2004), Using GOME NO<sub>2</sub> satellite data to examine regional differences in TOMCAT model performance, *Atmos. Chem. Phys.*, *4*(7), 1895–1912.
- Stevenson, D. S., R. M. Doherty, M. G. Sanderson, W. J. Collins, C. E. Johnson, and R. G. Derwent (2004), Radiative forcing from aircraft NO<sub>x</sub> emissions: Mechanisms and seasonal dependence, *J. Geophys. Res.*, *109*, D17307, doi:10.1029/2004JD004759.
- Stordal, F., et al. (2006), TRADEOFFS in climate effects through aircraft routing: Forcing due to radiatively active gases, *Atmos. Chem. Phys. Discuss.*, *6*(5), 10,733–10,771.
- Warwick, N. J., S. Bekki, K. S. Law, E. G. Nisbet, and J. A. Pyle (2002), The impact of meteorology on the interannual growth rate of atmospheric methane, *Geophys. Res. Lett.*, *29*(20), 1947, doi:10.1029/2002GL015282.
- Wild, O., K. S. Law, D. S. McKenna, B. J. Bandy, S. A. Penkett, and J. A. Pyle (1996), Photochemical trajectory modeling studies of the north Atlantic region during August 1993, *J. Geophys. Res.*, *101*(D22), 29,269–29,288.
- Wild, O., M. J. Prather, and H. Akimoto (2001), Indirect long-term global radiative cooling from NO<sub>x</sub> emissions, *Geophys. Res. Lett.*, *28*(9), 1719–1722.
- 
- O. Dessens, M. O. Köhler, J. A. Pyle, and H. L. Rogers, Centre for Atmospheric Science, Department of Chemistry, University of Cambridge, Lensfield Road, Cambridge CB2 1EW, UK. (olivier.dessens@atm.ch.cam.ac.uk; marcus.koehler@atm.ch.cam.ac.uk; john.pyle@atm.ch.cam.ac.uk; helen.rogers@atm.ch.cam.ac.uk)
- G. Rädcl and K. P. Shine, Department of Meteorology, University of Reading, Earley Gate, PO Box 243, Reading RG6 6BB UK. (g.radel@reading.ac.uk; k.p.shine@reading.ac.uk)
- O. Wild, Department of Environmental Science, Lancaster University, Lancaster, LA1 4YQ UK. (o.wild@lancaster.ac.uk)